Transp Porous Med (2013) 96:353–367
DOI 10.1007/s11242-012-0092-z

Selection Principle of Optimal Profiles for Immiscible Multi-Fluid Hele-Shaw Flows and Stabilization

Prabir Daripa · Xueru Ding

Received: 20 April 2012 / Accepted: 16 October 2012 / Published online: 26 October 2012

Abstract In this paper, we discuss a previously unknown selection principle of optimal viscous configurations for immiscible multi-fluid Hele-Shaw flows that have emerged from numerical experiments on three- and four-layer flows. Moreover, numerical investigation on four-layer flows shows evidence of four-layer systems which are almost completely stabilizing. Simple physical mechanisms that explain both of these findings are discussed.

Keywords Multi-layer Hele-Shaw flow · Porous media flow · Enhanced oil recovery · Linear stability · Optimal viscous profile

1 Introduction

We consider flows involving many distinct immiscible fluids in succession in a Hele-Shaw cell assuming sharp interfaces between different regions of fluids of distinct viscosity profiles. See Fig. 1 for example where there are only four layers. Such Hele-Shaw flows have been referred in all of our papers (Daripa 2008a,b, 2011; Daripa and Pasa 2006, 2007, 2010) as multi-layer (three-layer, four-layer, and so on) with slight abuse of the usage of the word "layer" perhaps. In a geoscience context, layer is generically attached to horizontal strata parallel to the imposed mean flow. However, we have been using the word "layer" to mean strata perpendicular to the imposed mean flow. In order to continue the tradition that has been set by our works in this area and not to confuse readers of our previous works on similar flows, we henceforth call these flows as multi-layer flows.

At the risk of oversimplification, multi-layer Hele-Shaw flows serve as models for immiscible displacement processes during enhanced oil recovery by injection of a sequence of fluids in a homogeneous porous media. The nuances of oversimplification and similarity

P. Daripa (✉)
Department of Mathematics, Texas A&M University, College Station TX 77843, USA
e-mail: daripa@math.tamu.edu; prabir.daripa@math.tamu.edu

X. Ding
Department of Petroleum Engineering, Texas A&M University at Qatar, Doha, Qatar

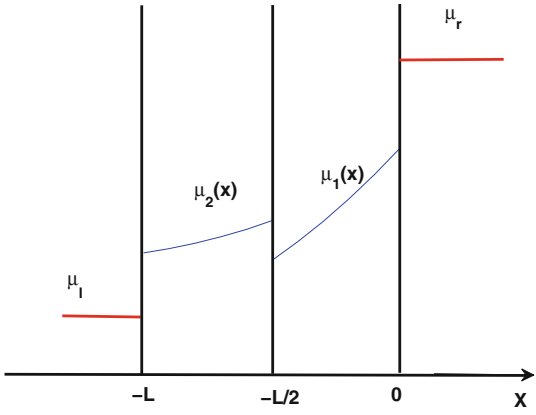

Fig. 1 Four-layer fluid flow in a Hele-Shaw cell

between Hele-Shaw and the porous media flows have been addressed before (see Daripa and Ding 2012; Daripa 2008a). In general, this displacement process is overall unstable and complexity of the instability, in its nascent and fully developed stages, usually depends on the viscous configuration of the system (i.e., the viscous profiles of different layers and jump in viscosity at each of the interfaces) and interfacial tensions. Fully developed stages containing fingers of displacing fluids is detrimental in the context of oil recovery due to early water breakthrough. Past several decades of research in this area have created a general consensus containing even the linearized growth rates of unstable waves curtail the severity of the fingering phenomena, thereby improving oil recovery. Therefore, one of the goals has been to develop injection schemes that will reduce the growth rate of the most dangerous wave as much as possible. The utopian goal in this area, of course, is to have an injection policy that completely stabilizes the flow which is perhaps impossible for heterogeneous porous media but may be possible to a large extent for Hele-Shaw flow which is a simplified model for homogeneous porous media flow.

It is well-known that an injection policy involving two-layer flows such as water displacing oil is an unstable process. Recent works of the authors and collaborators (see Daripa 2008b,a; Daripa and Ding 2012) reveal that such displacement processes can be stabilized to some extent using an injection policy in which two or more fluids having constant and/or monotonic viscous profiles (viscosity profile of each layer bounded by viscosities of the extreme layer fluids (oil and water)) are injected judiciously in succession. In Daripa (2008a), injection of an arbitrary number of fluids, each having constant viscosity, in succession has been considered and an estimate for the maximum growth rate has been obtained from stability analysis of the flow. There, use of this estimate as a guide to select an optimal injection policy (i.e., one having most stabilizing capacity measured by the smallest value of the maximum growth rate) has been shown. Similar multi-layer (or multi-fluid) flows when the fluids in various layers can have variable viscosity is too difficult to analyze theoretically (see Daripa 2008a) and too impractical to solve numerically due to excessive number of parameters. The simplest of these is the three-layer flow where the middle layer has variable viscosity profile and the other two fluid layers have constant viscosity fluids corresponding to oil and water. This case has been studied theoretically to the extent possible (see Daripa 2008a) and also numerically recently (see Daripa and Ding 2012). In this later article, authors use numerical results on optimal profiles to explain possible physical mechanisms behind the selection of optimal viscous profiles for the middle layer profile in the three-layer flows. In this paper, we

investigate this issue further using 4-layer flows and also explore the possibility of complete stabilization of 4-layer flows for some choices of viscous profiles of the internal layers. We keep this section short by directing readers to Daripa (2008a) and Daripa and Ding (2012) for a discussion of significance and relevance of optimal injection policies in the context of enhanced oil recovery including an historical account of other authors' contribution in this area.

This paper is laid out as follows. The mathematical model and the numerical procedure for the solution of the resulting eigenvalue problem are discussed in Sect. 2. In Sect. 3, numerical results are presented and discussed. Finally, we conclude in Sect. 4 by summarizing the main results.

2 Preliminaries and Formulation

The four-layer (or equivalently four-domain) Hele-Shaw flows with two internal layers is shown in Fig. 1. A fluid of viscosity μ_1 occupies an infinite region $x < -L$ and a fluid of viscosity $\mu_r > \mu_1$ occupies an infinite region $x > 0$. Two intermediate regions $-(L/2) < x < 0$ and $-L < x < -(L/2)$ have fluids of smooth viscous profiles $\mu_1(x)$ and $\mu_2(x)$, respectively. The interfacial tension at the three interfaces located at $x = 0, -L/2, -L$ are T_0, T_1, T_2, respectively. With application to enhanced oil recovery in mind, we assume that each of the two exterior interfaces at $x = -L$ and 0 can have positive viscosity jumps in the direction of flow, the middle interface can have viscosity jump but the viscosity on either side of the interface cannot be outside the range $[\mu_1, \mu_r]$. The viscosity profiles of both the internal layers are restricted to be linear in this study which include the constant viscosity layer as a special case. The viscous configuration within these constraints that gives the smallest maximum growth rate is sought for given values of the interfacial tensions.

The fluid flow in each domain is governed by

$$\nabla\cdot\mathbf{u} = 0, \quad \nabla p = -\mu\,\mathbf{u}, \quad \frac{D\mu}{Dt} = 0, \tag{1}$$

where $\nabla = \left(\frac{\partial}{\partial x}, \frac{\partial}{\partial y}\right)$ and $\frac{D}{Dt}$ is the material derivative. The first Eq. $(1)_1$ is the continuity equation for incompressible flow, the second Eq. $(1)_2$ is the Darcy's law (Darcy 1856), and the third Eq. $(1)_3$ is the advection equation for viscosity (Gorell and Homsy 1983; Daripa and Pasa 2005b). This last equation simply states that viscosity is simply advected by the fluid. Because of the analogy of this flow with flow in a Hele-Shaw cell, this model is commonly referred as the Hele-Shaw model. A description of this Hele-Shaw model can be found in Pearson (1977), Gorell and Homsy (1983), Pasa (2008), Daripa (2008a), and Daripa (2008b).

The above system (1) is subject to kinematic interfacial conditions, namely that particles on interfaces remain there, i.e., on an interface given by $x = \tilde{g}(y, t)$ in a moving frame, $\tilde{g}_t = \tilde{u}(0, y, t)$. Additionally, there are also dynamic boundary conditions on the interfaces, namely, that jump in pressure across an interface is balanced by local curvature times the interfacial tension, which within linear approximation for an interface $x = \tilde{g}(y, t)$ is given by $p^+(0) - p^-(0) = T\tilde{g}_{yy}$, where the superscripts "+" and "−" are used to denote the "right" and "left" limit values, T is the interfacial tension, and $\tilde{g}_{yy}$ is the approximate curvature of the perturbed interface. Details can be found in Daripa and Pasa (2004) and Daripa (2008a).

The system (1) admits a simple basic solution, namely the whole fluid set-up moves with speed U in the x direction and the two interfaces, namely the one separating the left layer from the middle-layer and the other separating the right layer from the middle-layer, are planar,

i.e., parallel to the y-axis. The pressure corresponding to this basic solution is obtained by integrating $(1)_2$. In a frame moving with velocity $(U, 0)$, the above system is stationary. Here and below, with slight abuse of notation, the same variable x is used in the moving reference frame. In linearized stability analysis by normal modes, disturbances (denoted by tilde variables below) in the moving reference frame are written in the form

$$(\widetilde{u}, \widetilde{v}, \widetilde{p}, \widetilde{\mu}) = (f(x), \psi(x), \phi(x), h(x))e^{(iky+\sigma t)} \tag{2}$$

where k is the wave number and σ is the growth rate. We then insert this disturbance form into the linearized disturbance equations obtained from (1) and also into the linearized dynamic and kinematic interfacial conditions (see Daripa and Pasa 2005a). After some algebraic manipulation, we obtain the following equations

$$\left.\begin{array}{ll} -(\mu_1 f_x)_x + k^2\mu_1 f = \lambda k^2 U \mu_{1x} f, & x \in (-L/2, 0), \\ -(\mu_2 f_x)_x + k^2\mu_2 f = \lambda k^2 U \mu_{2x} f, & x \in (-L, -L/2), \\ f_{xx} - k^2 f = 0, & x \notin (-L, 0). \end{array}\right\} \tag{3}$$

and the boundary conditions

$$\left.\begin{array}{l} f_x(0) = (\lambda e + q) f(0), \\ \mu_1(-L/2) f_x^+(-L/2) - \mu_2(-L/2) f_x^-(-L/2) = -\lambda E_1 f(-L/2), \\ f_x(-L) = (\lambda r + s) f(-L), \end{array}\right\} \tag{4}$$

where $\lambda = 1/\sigma$ and e, q, r, s are defined by

$$\left.\begin{array}{l} e = \{(\mu_r - \mu(0))Uk^2 - T_0 k^4\}/\mu(0),\ q = -\mu_r k/\mu(0) \le 0, \\ r = \{(\mu_1 - \mu(-L))Uk^2 + T_2 k^4\}/\mu(-L),\ s = -\mu_1 k/\mu(-L) \ge 0, \\ E_1 = k^2 U(\mu_1(-L) - \mu_2(-L)) - k^4 T_1. \end{array}\right\} \tag{5}$$

The weak formulation of this problem was analyzed in Sect. 7 of Daripa (2008a), where it was conjectured from an upper bound estimate of the growth rate, that four-layer flows could be a candidate for complete stabilization with some monotonic viscous profiles of the type shown in Fig. 1. Below, we investigate the possibility of complete stabilization numerically. The governing differential Eqs. $(3)_1$ and $(3)_2$ and boundary conditions (4) are discretized over the domain $(-L, 0)$ using $2M + 1$ uniformly spaced nodes. Then the discrete analog of the above problem can be written as

$$A'\mathbf{f} = \lambda B'\mathbf{f}, \tag{6}$$

where A' and B' are square matrices of size $(2M + 1) \times (2M + 1)$ and $\mathbf{f}$ is the vector with entries $f_0, f_1, f_2, \ldots, f_{2M}$. The above system is solved numerically for λ from which the growth rate $\sigma = 1/\lambda$ is obtained.

For parameters $\mu_1, \mu_r, U, L, T_0, T_1$, and T_2 fixed, the growth rate σ then depends on k and the viscous profiles $\mu_1(x)$ and $\mu_2(x)$ of two layers. If we restrict our studies with linear viscous profiles, then the viscous profile $\mu_1(x)$ is completely defined by $\mu_1(-L/2)$ and its slope, say α_1. Similarly the viscous profile $\mu_2(x)$ is completely defined by $\mu_2(-L/2)$ and its slope, say α_2. Thus, the growth rate σ of a disturbance with wave number k in general depends on k, $\mu_1(-L/2)$, $\mu_2(-L/2)$, α_1, and α_2. Below we use several terminology whose meaning should be clear in the context. But to avoid any confusion, we define these here. The maximum growth rate $\sigma_{\max}$ refers to the growth rate of the most dangerous wave number for a given choice of viscous profiles, i.e., for given values of $\mu_1(-L/2)$, $\mu_2(-L/2)$, α_1, and α_2. Thus $\sigma_{\max}$ depends on $\mu_1(-L/2)$, $\mu_2(-L/2)$, α_1, and α_2. Below, minimized maximum growth rate refers to the minimum value of $\sigma_{\max}$, minimum taken over all allowable

values of the slopes, α_1 and α_2, of two linear profiles. This minimized maximum growth rate still depends on the values of $\mu_1(-L/2)$ and $\mu_2(-L/2)$. Similarly, the smallest minimized maximum growth rate means the minimum value of minimized maximum growth rate, minimum taken over all allowable values of $\mu_1(-L/2)$ and $\mu_2(-L/2)$. The viscous profiles of the two layers corresponding to the smallest minimized maximum growth rate together with the constant viscous profiles of two external layers constitute the optimal viscous configuration of the system because it will be the most stabilizing of all linear viscous configurations. Thus "smallest minimized maximum growth rate" means the same as "maximum growth rate of the optimal viscous configuration." Below, we use the terminology "maximum growth rate of the optimal configuration" instead of "smallest minimized maximum growth rate."

Since interfacial tensions are generally stabilizing specially for the long waves, it is conceivable that stabilizing (destabilizing) viscous profiles, large enough interfacial tensions, and destabilizing (stabilizing) interfacial viscosity jumps can together drastically stabilize the system. We can find merits of this speculation by numerical simulation which we do in the next section. Purpose of numerical simulations is then to (i) seek such optimal viscous configuration and determine its dependency on the interfacial tensions; (ii) identify emergence of drastically stabilized flow and corresponding viscous configuration and interfacial tensions; and (iii) identify common features, if any, between optimal viscous configurations for the four-layer case and for the previously reported (see Daripa and Ding 2012) three-layer case. As we will see, we identify the selection principle of optimal viscous configuration that may as well hold for multi-layer (more than 4-layer) Hele-Shaw flows with small and large slug sizes.

3 Results and Discussion

All simulations are performed with linear viscous profiles in each of the two internal layers for the four-layer case. This allows comparison with the results on three-layer linear profile case reported in Daripa and Ding (2012) so long as the other parameter values are chosen to be the same, which we do. Simulations for different values of interfacial tensions while keeping the other parameters same as for the three-layer case, namely $\mu_l = 2$, $\mu_r = 10$, $L = 1$, $U = 1$, are carried out.

The first simulation is carried out with interfacial tensions same as in the three-layer case (see Daripa and Ding 2012), namely $T_0 = T_1 = T_2 = 2/3$ with $\sum T_i = 2$. Figure 2 shows minimized maximum growth rate $\sigma_{\max}$ versus $\mu_1(-L/2)$ and $\mu_2(-L/2)$ in two different formats, the left panel in standard line plots and the right panel in color grid plot. For each pair of $(\mu_1(-L/2), \mu_2(-L/2))$, the minimized maximum growth rate is obtained from simulating over all of the parameter combinations of $\mu_1(0) \in [2, 10]$ and $\mu_2(-L) \in [2, 10]$. From this figure, we find that $\sigma_{\max} = 0.3622$ for the optimal profile. For this optimal profile we find $\mu_1(-L/2) = 5$ and $\mu_2(-L/2) = 4$. The other two corresponding viscosity values are $\mu_2(-L) = 4$ and $\mu_1(0) = 5$. Comparing with the optimal profile for three-layer case reported in Daripa and Ding (2012), $\sigma_{\max} = 0.3652$.

Thus, the four-layer and the three-layer flows with optimal viscous profiles are more or less equally unstable for the above choices of parameters. The optimal viscous profiles for the three-layer and the four-layer are shown in Fig. 3. We will be focusing exclusively on the four-layer case henceforth. It is expected based on stability theory that increasing interfacial tensions should be stabilizing for the flows and perhaps with high enough interfacial tensions, the flows can be drastically stabilized. But it is perhaps difficult to predict the rate at which

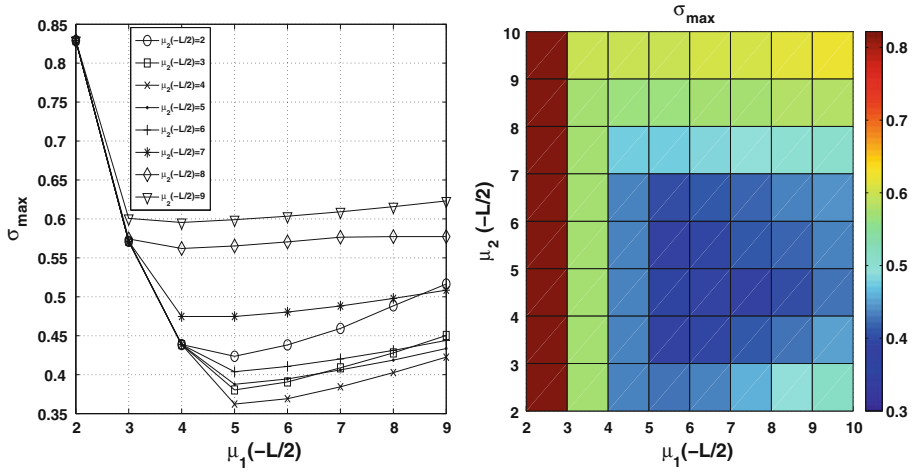

Fig. 2 Minimized $\sigma_{\max}$ versus $\mu_1(-L/2)$ for various values of $\mu_2(-L/2)$, while both $\mu_2(-L)$ and $\mu_1(0)$ are varying from 2 to 10. The viscous profiles $\mu_1(x)$ and $\mu_2(x)$ are both linear. All the other parameters are: $\mu_1 = 2$, $\mu_r = 10$, $T_0 = T_1 = T_2 = 2/3$, $U = 1$, $L = 1$, and $2M + 1 = 31$

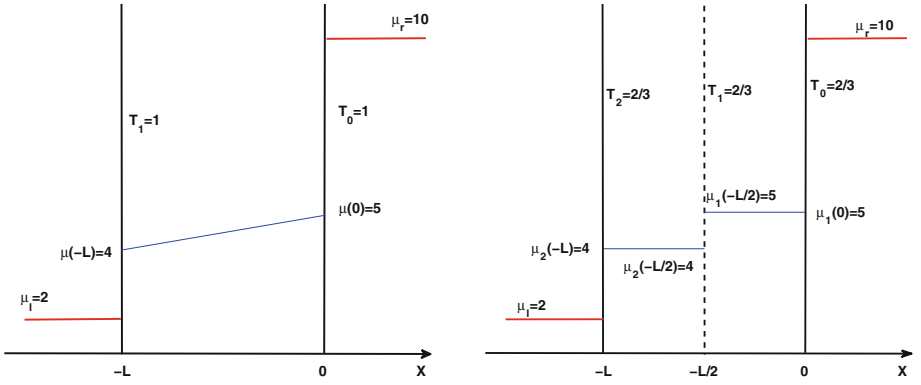

Fig. 3 Optimal viscous profiles in three-layer and four-layer Hele-Shaw flows

the growth rate decreases with increasing interfacial tensions. Next set of simulations are carried out to find answers to these issues.

We carry out simulations with interfacial tensions $T_0 = T_2 = 1$ and vary the interfacial tension T_1. Figure 4 shows $\sigma_{\max}$ of the optimal profile versus the interfacial tension T_1. It is important to emphasize that the optimal profile also depends on the value of T_1. It is clear that the maximum growth rate decreases with increasing interfacial tension T_1. Furthermore, the maximum growth rate decreases very rapidly with T_1 initially, i.e., when T_1 is small and reaches a plateau for large T_1, specially for $T_1 > 100$ (approximately). It is interesting to note that when T_1 is close to zero, for the optimal profile $\sigma_{\max} = 0.3673$ which is close to $\sigma_{\max} = 0.3652$, the maximum growth rate for the optimal linear profile in the three-layer case (see Daripa and Ding 2012). We see from this figure that almost complete stabilization requires unusually high interfacial tension of the middle interface while interfacial tensions of the other two interfaces have the modest values, namely $T_0 = T_2 = 1$.

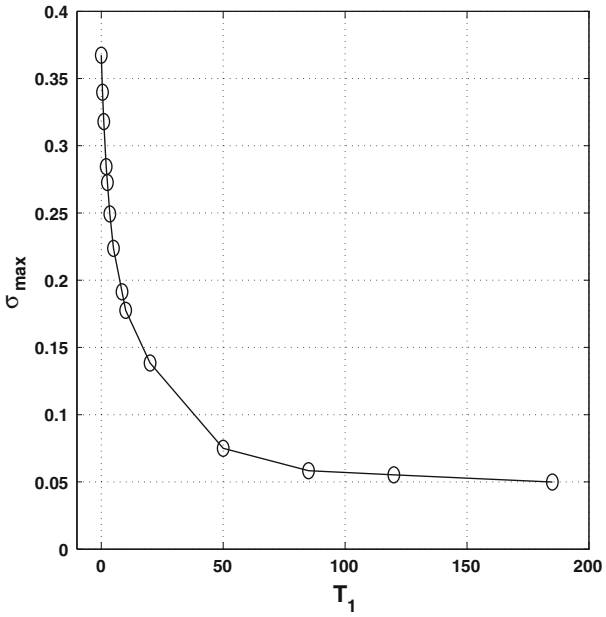

Fig. 4 Maximum growth rate $\sigma_{\max}$ of the optimal profiles versus T_1.$\mu_1(0) \in [2, 10]$, $\mu_2(-L) \in [2, 10]$. Viscous profiles $\mu_1(x)$ and $\mu_2(x)$ are both linear. All the other parameters are: $\mu_1 = 2$, $\mu_r = 10$, $T_0 = T_2 = 1$, $U = 1$, $L = 1$, and $2M + 1 = 31$

Most of our results shown have been obtained with 31 number of grid points and refining the mesh does not change the results. The overriding conclusions from our study based on these grid points remain same as with finer grid size. In support of this, plots of $\sigma_{\max}$ versus T_1 for four different grid sizes are shown in Fig. 5. We see the convergence of the plots as mesh is refined. The inset shows excellent agreement between results obtained with grid points 31 and 41.

Figure 6 shows six optimal viscous configurations associated with Fig. 4. Different panels in this figure correspond to different range of values for T_1. Top left panel corresponds to $T_1 = 0.5$, top right panel corresponds to $1 \leq T_1 < 8$, and so on. We see that viscosity in each layer is constant with positive jump (in the direction of displacement) in viscosity at each of the interfaces. It should be mentioned here that characterization of these viscous profiles are approximate due to numerical error. The viscosity jump at the middle interface increases monotonically and that at each of the exterior interfaces decreases monotonically with increasing values of T_1. Figure 7 shows the plot of viscosity jumps at the middle interface versus T_1. It shows that the jump in viscosity approaches zero as T_1 approaches zero. The observations made from Figs. 4, 6, and 7 can be explained qualitatively as follows which is similar, but more involved, to our discussion for the three-layer case (see Daripa and Ding 2012). Next, we show the optimal viscous configurations of the set-up for several values of the interfacial tension T_1.

In general, there is an interplay between interfacial modes and the fingering (instability in the layer) modes that determines the optimum viscous configuration of such multi-layer systems. The interfacial and layer instabilities contribute toward the overall instability of the system as measured by $\sigma_{\max}$. Increasing interfacial tension provides stabilization of a flow, which is reflected in this problem through a decrease in the value of $\sigma_{\max}$ (see Fig. 4); this

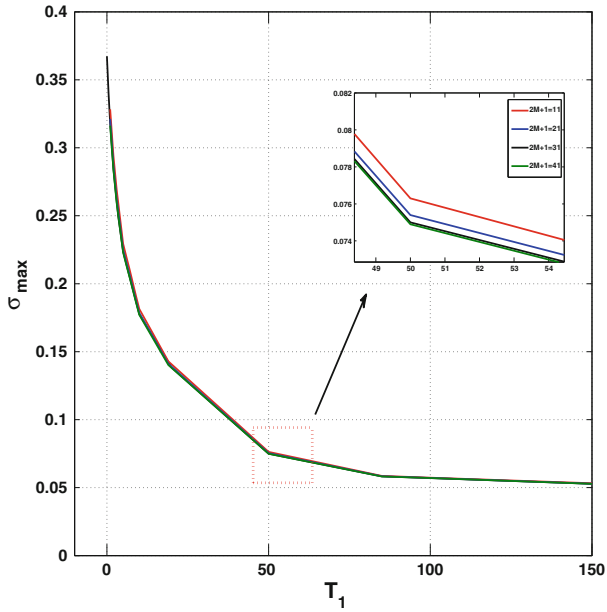

Fig. 5 Convergence study: maximum growth rate $\sigma_{\max}$ of the optimal profiles versus T_1 for four different number of grid points: $2M + 1 = 11, 21, 31, 41$. Rest of the data are same as in Fig. 4

reduction must be shared by all instability modes (interfacial and layer) present. Since only the middle interface would be stabilized by an increase in T_1 if it were not for the other two interfaces, a transfer of stability from the middle interface to the other two interfaces must take place. This is naturally accomplished by a decrease in the viscosity jumps at both the exterior interfaces and an increase in the viscosity jump at the middle interface. However, this should occur in a way so that the maximum value of $\sigma_{\max}$ is minimum among all possible configurations since an optimal configuration is sought in these calculations. This explains the changes in the optimal configuration (see Fig. 6) that take place with increasing T_1. In particular, it appears from the interfacial viscosity jumps in the optimal configurations shown in Fig. 6 that splitting of the net gain in stabilization (due to an increase in T_1) among three interfacial modes occurs along the equipartition principle in a qualitative and approximate sense. It is worth recalling that this same principle explains selection mechanism of the optimum configurations in the case of three-layer Hele-Shaw flows (Daripa and Ding 2012). It is conjectured here that this same principle will be at work for more than four-layer flows as well.

The rational explanation given above behind the selection principle of optimal configurations in Fig. 6 should help predict the direction in which the viscosity jumps at various interfaces should occur (i.e., increase or decrease) in response to changes in one or more interfacial tensions. It is difficult to predict a priori whether the optimal viscous profile of each layer will be a constant or a linear viscous profile, keeping in mind that optimal profiles are sought only with linear profiles of which, constant viscous profile is a special case. The next set of experiments is designed to exemplify this and to show the possibility of drastic, almost complete, stabilization of four-layer flows.

In this last set of simulations, we keep interfacial tension $T_1 = 1$ and increase the values of the other two interfacial tensions T_0 and T_2 keeping $T_0 = T_2$. Figure 8 shows the maximum

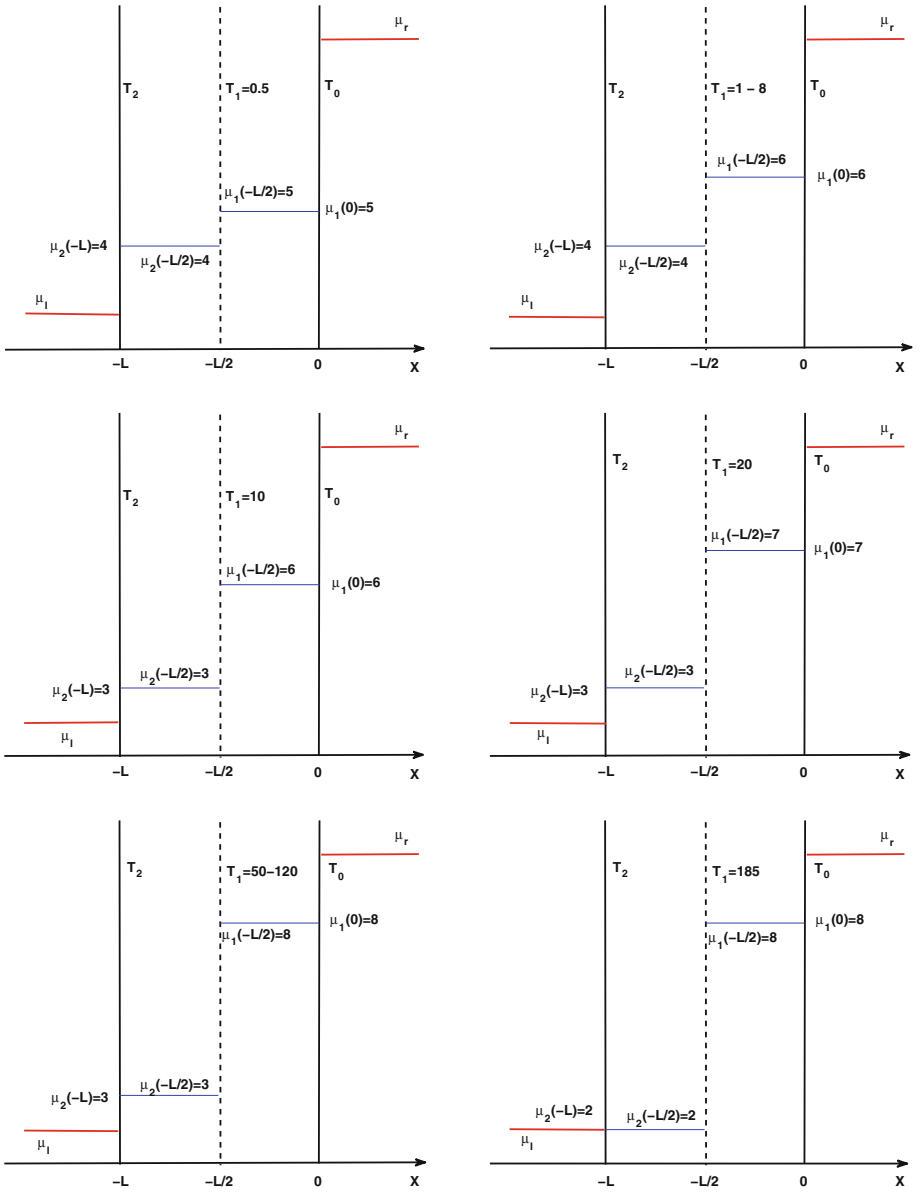

Fig. 6 Optimal viscosity profiles for different values of T_1. The parameters are: $\mu_1 = 2$, $\mu_r = 10$, $T_0 = T_2 = 1$, $U = 1$, $L = 1$, and $2M + 1 = 31$

growth rates of the optimal profiles versus interfacial tensions $T_0 = T_2$. This figure shows that the maximum growth rate decreases with increasing values of $T_0 = T_2$ which is expected. Two interesting observations are worth paying attention to: (i) dramatic stabilization capacity of interfacial tensions of exterior interfaces. Increasing values of $T_0 = T_2$ from 1 to 10 stabilizes the flow in excess of two-fold as seen in Fig. 8. The corresponding optimal viscous configurations are shown in the top two right panels of Fig. 9. Similar, but slightly less,

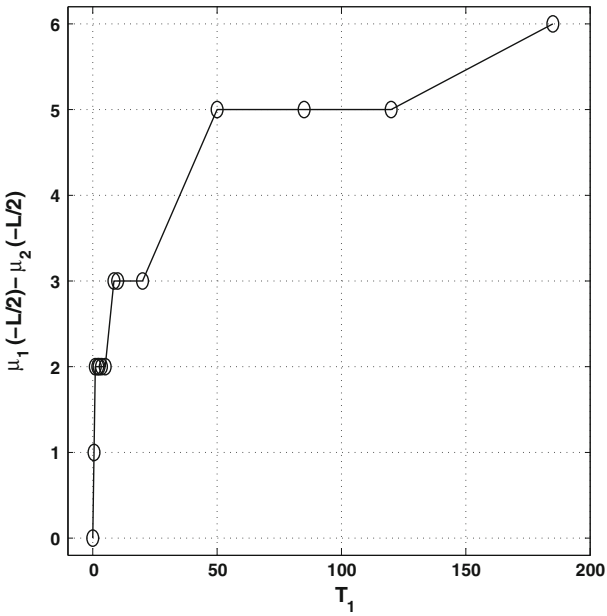

Fig. 7 The viscosity jumps $\mu_1(-L/2) - \mu_2(-L/2)$ versus $T_1.\mu_1(0) \in [2, 10]$, $\mu_2(-L) \in [2, 10].\mu_1(x)$ and $\mu_2(x)$ are both linear. All the other parameters are: $\mu_1 = 2$, $\mu_r = 10$, $T_0 = T_2 = 1$, $U = 1$, $L = 1$, and $2M + 1 = 31$

dramatic stabilization of interfacial tension of the middle interface is also seen in Fig. 4; (ii) With increasing values of $T_0 = T_2$, maximum growth rate of the optimal profile approaches to infinitesimally small value as expected. Interestingly, the flow with the optimal viscous configuration is almost stable when $T_0 = T_2 = 100$. Even though, such dramatic effect of high interfacial tensions on stabilization is expected on theoretical ground, the selection principle of optimal viscous configurations that make such dramatic stabilization possible is not well understood. We discuss this next.

Figure 9 shows optimal viscous configurations for different values of $T_0 = T_2$. The changes in optimal configurations with changes in the values of $T_0 = T_2$ can be partly explained using the selection principle discussed above. For low values of $T_0 = T_2$, interfacial modes exist (see left top panel in Fig. 9) which we have seen in one of the panels (top right) in Fig. 6. With increasing values of $T_0 = T_2$, jumps in viscosity at exterior interfaces must increase to offset part of the gain in stabilization of these interfaces due to increase in their interfacial tensions. This also results in a decrease of viscosity jump at the middle interface (see Fig. 9) thereby providing some stabilization of the middle interface; thus allows overall stabilization of the system as well as of the individual interfaces. This trend towards selection of optimal profiles due to increasing values of $T_0 = T_2$ brings stabilization of all three interfacial modes and hence lower maximum growth rate of the flow as expected from stability theory. The viscosity jump $\mu_1(-L/2) - \mu_2(-L/2)$ at the interior interface decreases continuously with increasing $T_0 = T_2$, going from positive to negative values. This dependency is shown in Fig. 10. However, our selection principle cannot explain the transition from constant to linear profiles of optimal viscous configurations seen in Fig. 9. We see that the viscous profile in each layer is constant (linear) if the interfacial viscosity jump, $\mu_1(-L/2) - \mu_2(-L/2)$, at the internal layer in the direction of basic flow is positive (negative).

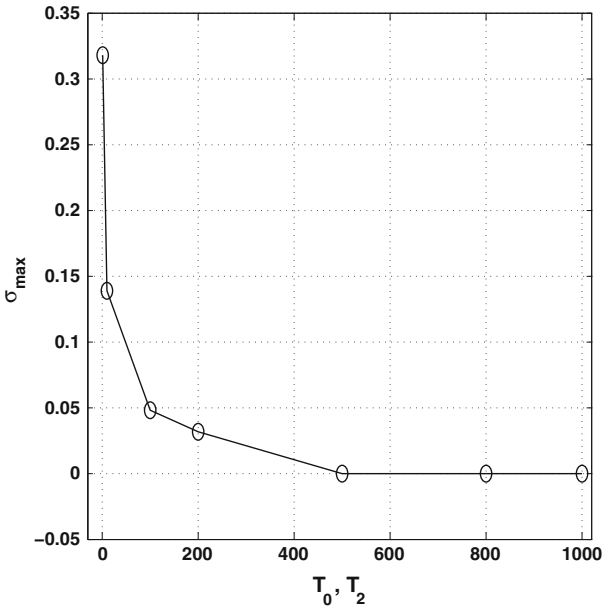

Fig. 8 Maximum growth rate $\sigma_{\max}$ of optimal profiles versus T_0 and T_2.$\mu_1(0) \in [2, 10]$, $\mu_2(-L) \in [2, 10]$.$\mu_1(x)$ and $\mu_2(x)$ are both linear. All the other parameters are: $\mu_1 = 2$, $\mu_r = 10$, $T_1 = 1$, $U = 1$, $L = 1$, and $2M + 1 = 31$

Interestingly, with increase in interfacial tensions $T_0 = T_2$, constant optimal profiles (middle left panel of Fig. 9) first become linear optimal profiles (middle right panel of Fig. 9) with no jump in viscosity at the middle interface. With further increase in $T_0 = T_2$ the middle interfacial mode and the two fingering or layer modes become individually stable. We see that the four-layer flows with linear optimal viscous profiles of the two layers shown in the three panels of this figure are almost completely stabilizing as seen in Fig. 8. In Daripa (2008a), it was speculated that complete stabilization of four-layer flows are possible for certain types of viscous configurations such as the one shown in Fig. 1. It turns out that four-layer flows with such viscous configurations as in Fig. 1 are stable. Instead, four-layer flows with different types of viscous configurations (e.g., bottom two panels of Fig. 9) are found to be almost completely stabilizing provided the interfacial tensions are very high.

4 Conclusions

Hydrodynamic stability of an immiscible displacement process involving an arbitrary number of fluids each having a constant viscosity has been recently studied in Daripa (2008a). The effect of constant viscosities of various fluids and the interfacial tensions on stabilization of the system is now reasonably well understood from this work. From the view point of Enhanced Oil Recovery (EOR), it is more useful to study the case when the fluids in various layers of finite length (slug size) can have arbitrary monotonic viscous profiles and arbitrary interfacial tensions. In this context, it is a challenging problem to find the optimal viscous configuration which has a maximum stabilizing capacity, in particular the one that completely

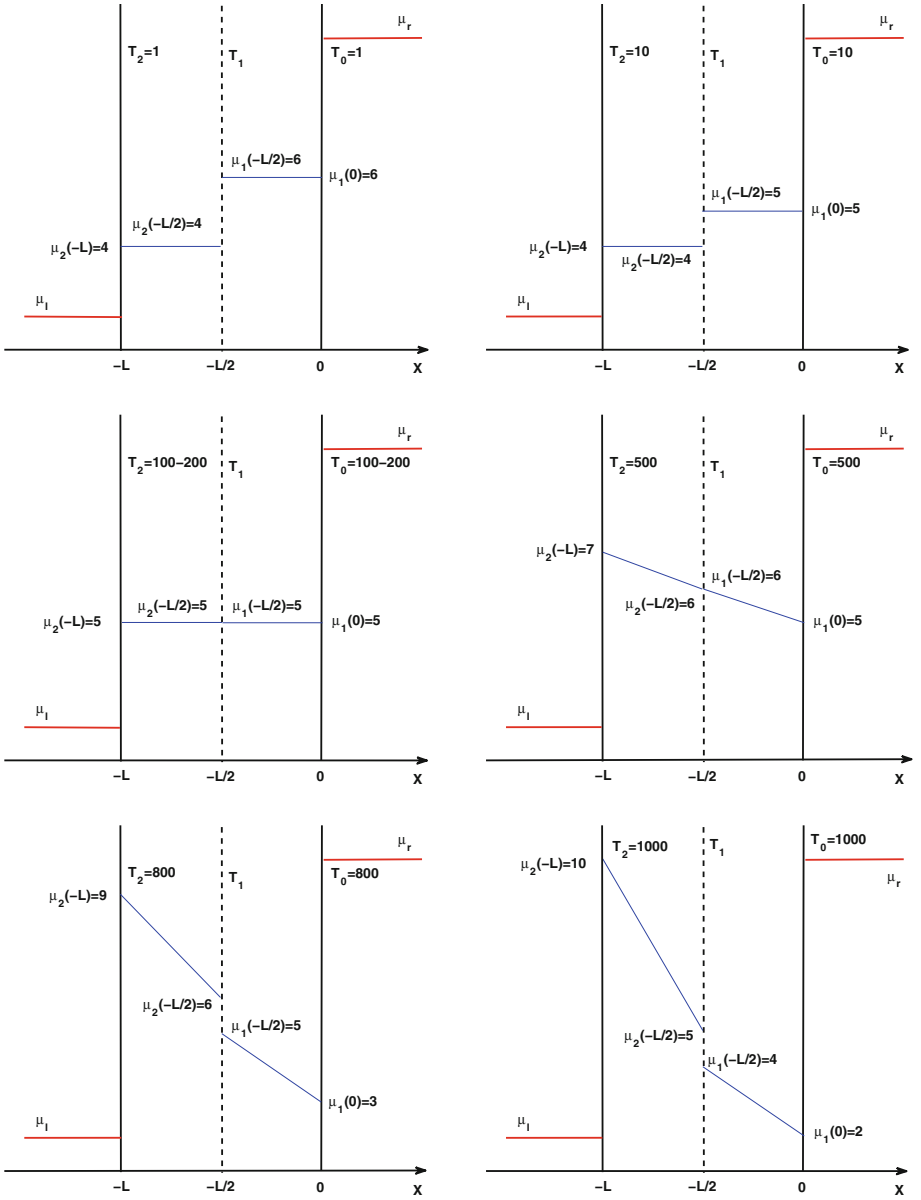

Fig. 9 Optimal viscosity configurations for different values of $T_0 = T_2$. The parameters are: $\mu_l = 2$, $\mu_r = 10$, $T_1 = 1$, $U = 1$, $L = 1$, and $2M + 1 = 31$

stabilizes an otherwise unstable multi-layer flow in the event that such a configuration exists. Even more challenging problem is to find the principle (physical mechanisms) behind the selection of the most optimal viscous configuration for multi-layer Hele-Shaw flows. In this paper, we have addressed both of these problems.

Recently, we (see Daripa and Ding 2012) numerically addressed the physical mechanisms behind the selection of optimal viscous configuration in the case of three-layer Hele-Shaw

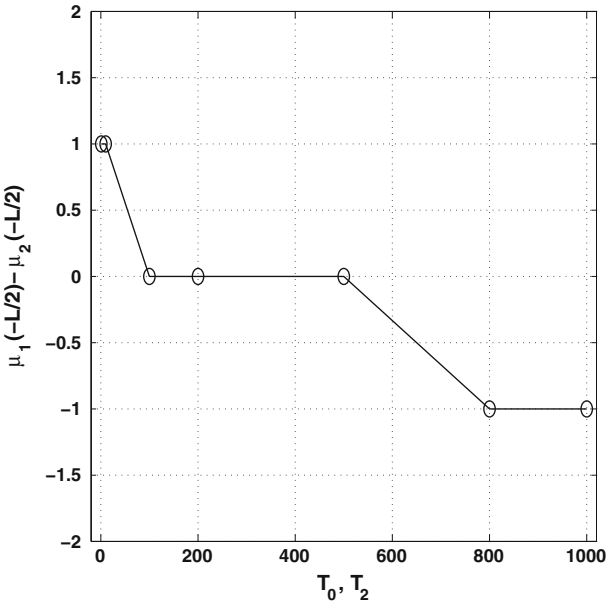

Fig. 10 $\mu_1(-L/2) - \mu_2(-L/2)$ versus T_0 and T_2 for the viscous profiles shown in Fig. 9. $\mu_1(0) \in [2, 10]$, $\mu_2(-L) \in [2, 10]$.$\mu_1(x)$ and $\mu_2(x)$ are both linear. All the other parameters are: $\mu_1 = 2, \mu_r = 10, T_1 = 1, U = 1, L = 1$, and $2M + 1 = 31$

flows. The study presented here is an extension of that work to the four-layer flows. Results on the four-layer flows with constant viscosity layers supports, in most but not all instances, the following selection principle of optimal unstable viscous configuration: namely, optimal unstable viscous configuration of multi-layer Hele-Shaw flows with constant viscosity layers results from approximate equi-distribution of the net instability of the system among interfacial modes. When internal layers are allowed to have arbitrary linear viscous profiles, a clear selection principle that applies universally is not so obvious as we have seen in many numerical examples presented in the previous section. It is conjectured here that this selection principle for the most optimal unstable viscous configuration may be universal for multi-layer Hele-Shaw flows with an arbitrary number of interfaces. A second part of the selection principle which emerges from our numerical studies is about the selection of a new optimal unstable viscous configuration in response to a change in one or more of the interfacial tensions of an existing optimal unstable viscous configuration. This part of the selection principle states that for an optimal unstable viscous configuration with a fixed $(\mu_r - \mu_l)$, a change in any interfacial tension value induces an appropriate change in the corresponding interfacial viscosity jump to offset its effect on the individual interfacial stability of that interface resulting in a new optimal unstable viscous configuration. More research and numerical experiments are required to refine both parts of this selection principle.

Notice that this selection principle is qualitative in nature. It is difficult to predict the scope and broad application potential of this principle. One of the application areas is of course EOR where this principle, in conjunction with other prevailing criteria, can be used in decision making process for designing an optimal injection policy. For example, if one had to change one of the displacing fluids in an existing optimal multi-fluid injection policy

for economic or any other reason, then this principle can be used judiciously to choose such a fluid from a list of available fluids to maximize oil recovery by devising a new optimal injection policy. Depending on the choice of the fluid, the interfacial tensions of both the interfaces bounding this fluid layer may change. If this change is positive (negative) for one of these two interfaces, then the above selection principle suggests that the viscosity of the fluid should be such that viscosity jump at that interface increases (decreases); similarly for the other interface. The problem here is that process of application to home in the right fluid is iterative since interfacial tension depends on the fluid used. There should a wide variety of fluids to select from to make this work. This application idea just alluded is very primitive and it is obvious that it needs refinement through further research to solidify the application process of this principle. Exploring where and how to apply this selection principle successfully in an efficient and user-friendly manner is a topic of research in itself which falls outside the scope of this paper. For now, it is left up to the readers and users of this EOR technology to find the application of this principle.

A second contribution of this article is the possible existence of a viscous configuration that may completely, or almost completely, stabilize a four-layer Hele-Shaw flow with a net positive viscosity jump in the direction of flow. This issue has been investigated here. Numerical investigations to address this issue were motivated due to a conjecture made in Daripa (2008a) about possible existence of stable viscous configurations in such flows. As shown in this paper, almost stable viscous configurations (with a net positive viscosity jump in the direction of flow) exist provided the interfacial tensions are quite high. However, such stable configurations (see Figs. 9, 10) are not same as the ones (see Fig. 1) which were originally conjectured to be stable in Daripa (2008a). Very high interfacial tensions associated with the most stabilizing (almost stable) configurations are unusual in practical applications. Therefore, it is not possible in practice to have an almost completely stable viscous configuration for multi-layer Hele-Shaw flows within the restrictions of the viscous profiles mentioned in the opening paragraph of Sect. 2. However, multi-layer Hele-Shaw flows with some of the viscous configurations that provide significant stabilization (e.g., see Figs. 6, 9) can be set-up in practice. Finally, it is worth pointing out that this study provides a broad understanding of the above two main issues namely, selection principle of optimal viscous configuration and possibility of viscous configurations that almost completely stabilize the flow.

In closing, we want to mention current limitations of the selection principle, its applicability for oil industry, and future directions of this research. First of all, our study here concerns the rectilinear flow. In practice, flooding a reservoir with multiple fluid phases in succession from a well usually involves radial flow. The effect of radial nature of the flow, specially near the well, on this selection principle has not been investigated. It needs to be addressed by further study. It is worth pointing out the relevance of our results for heterogeneous reservoir. Toward this end, we want to emphasize that the mean flow direction in this study is perpendicular to the layers and not parallel as has been mentioned in Sect. 1. There have been studies of flow of this later type (see Artus et al. 2004; Daripa et al. 1988; Loggia et al. 1996) in heterogeneous porous media where the layers are of different permeability, a situation completely different and unrelated to the present study. It is mentioned here merely for the readers' benefit.

Acknowledgments This paper has been made possible by an NPRP Grant # 08-777-1-141 from the Qatar National Research Fund (a member of the Qatar Foundation). The statements made herein are solely the responsibility of the author. The authors wish to thank two anonymous reviewers and the editor for their constructive criticisms which have resulted in a much improved manuscript.

References

Artus, V., Netinger, B., Ricard, L.: Dynamics of the water–oil front for two-phase, immiscible flow in heterogeneous porous media. 1—stratified media. Transp. Porous Media **56**, 283–303 (2004)

Darcy, H.: Les Fontaines Publiques de la ville de Dijon. Paris (1856)

Daripa, P.: Hydrodynamic stability of multi-layer Hele-Shaw flows. J. Stat. Mech. **12**, 28 (2008a)

Daripa, P.: Studies on stability in three-layer Hele-Shaw flows. Phys. Fluids. **20**:Article No. 112101 (2008b)

Daripa, P.: On estimates for short wave stability and long wave instability in 3-layer Hele-Shaw flows. Phys. A **390**, 3069–3076 (2011)

Daripa, P., Ding, X.: A numerical study of instability control for the design of an optimal policy of enhanced oil recovery by tertiary dispalcement processes. Transp. Porous Media **93**(3), 675–703 (2012)

Daripa, P., Pasa, G.: An optimal viscosity profile in enhanced oil recovery by polymer flooding. Int. J. Eng. Sci. **42**(19–20), 2029–2039 (2004)

Daripa, P., Pasa, G.: New bounds for stabilizing Hele-Shaw flows. Appl. Math. Lett. **18**(11), 1293–1303 (2005a)

Daripa, P., Pasa, G.: On the growth rate for three-layer Hele-Shaw flows: variable and constant viscosity cases. Int. J. Eng. Sci. **43**(11–12), 877–884 (2005b)

Daripa, P., Pasa, G.: A simple derivation of an upper bound in the presence of a viscosity gradient in three-layer Hele-Shaw flows. J. Stat. Mech. 11 pp (2006). doi:10.1088/1742-5468/2006/01/P01014

Daripa, P., Pasa, G.: Stabilizing effect of diffusion in enhanced oil recovery and three-layer Hele-Shaw flows with viscosity gradient. Transp. Porous Media **70**, 11–23 (2007)

Daripa, P., Pasa, G.: On diffusive slowdown in three-layer Hele-Shaw flows. Q. Appl. Math. LXVIII:591–606 (2010)

Daripa, P., Glimm, J., Lindquist, B., Maesumi, M., McBryan, O.: On the simulation of heterogeneous petroleum reservoirs. In: Wheeler, M. (ed.) Numerical Simulation in Oil Recovery, IMA Vol. Math. Appl. 11, pp. 89–103. Springer, New York (1988)

Gorell, S.B., Homsy, G.M.: A theory of the optimal policy of oil recovery by the secondary displacement process. SIAM J. Appl. Math. **43**, 79–98 (1983)

Loggia, D., Rakotomalala, N., Salin, D., Yortsos, Y.C.: Phase diagram of stable miscible displacements in layered porous media. Europhys. Lett. **36**(2), 105–110 (1996)

Pasa, G.: Hele-Shaw flows. Math. Rep. **10**(2), 169–183 (2008)

Pearson, J.J.: The stability of some variable viscosity flows with application to oil extraction. unpublished, Cambridge University Report (1977)